Design of Substrate Integrated Waveguide Components Using Mode-Matching Techniques

Zamzam Kordiboroujeni and Jens Bornemann

Department of Electrical and Computer Engineering, University of Victoria, Victoria, BC, V8W 2Y2 Canada

***Abstract* — A simple, yet efficient mode-matching technique (MMT) is presented for the analysis and design of substrate integrated waveguide (SIW) circuits. The computational domain is formed by a rectangular box of electric and magnetic walls within which square via holes can be arbitrarily moved during an optimization process. The small substrate height limits the modes to those of the TE_{m0}-mode set. In order to adapt to common fabrication facilities, in which circular via holes rather than square ones are used, a simple conversion formula is introduced. Two examples of quasi-elliptic filters are presented. The excellent agreement of responses from the MMT with square vias and CST with circular vias validates the analysis and design procedure.**

***Index Terms* — Mode-matching techniques, substrate integrated waveguide, computer-aided design.**

I. Introduction

Over the last decade, substrate integrated waveguide (SIW) circuitry has evolved into a mature technology that is increasingly used by industry in commercial applications. In most cases, however, SIW components are designed using commercial full-wave solvers that require extensive computation times if optimization involves the iterative movement of a large number of via holes on the board.

Therefore, it is not surprising that other attempts have been made to accelerate the analysis and design process of SIW components. In order to determine the propagation characteristics, Floquet's theorem is usually used in combination with a numerical technique, e.g. [1], and parameter extraction is performed with the domain-decomposition FDTD [2]. Passive SIW components are analyzed with a variety of methods including – to name only a few - the finite-element time-domain (FETD) technique [3], the method of moments (MoM) [4, 5], the boundary integral-resonant mode expansion (BI-RME) method [6, 7], and combinations of the mode-matching technique (MMT) with the MoM [8, 9] or the spectral-domain approach (SDA) [10].

This paper adds to numerical techniques for SIW circuits an efficient MMT procedure that is based on via holes with initially square cross section. That makes the method fast and flexible. Then, in order to comply with standard circular-via PCB fabrication techniques, a conversion from square to circular via holes is performed.

II. Theory

Fig. 1 shows the top view of an SIW structure with square vias. The computational domain is limited by top and bottom electric as well as left and right (not shown) magnetic walls. Input ports are selected as dielectric-filled waveguides whose widths correspond to the equivalent widths of the SIW closest to the port [11]. In order to set up an MMT routine, we have to distinguish between three different scenarios as pointed out in Fig. 1 at locations A, B and C.

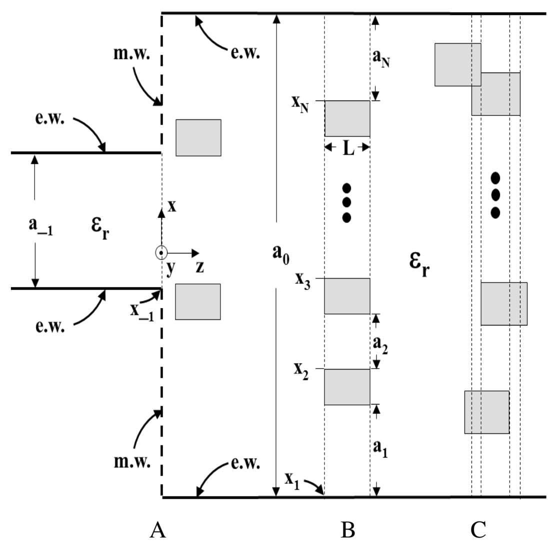

Fig. 1. Top view of SIW structure with square vias.

Using the set of TE_{m0} modes, the vector potential in each region of Fig. 1 can be expressed as:

$$A_{hz}^{\nu} = \sum_m \sqrt{Z_{hm}^{\nu}} \underbrace{\frac{a_\nu}{m\pi}\sqrt{\frac{2}{a_\nu b}}\cos\left\{\frac{m\pi}{a_\nu}\left(x - x_\nu\right)\right\}}_{T_{hm}^{\nu}(x)} \cdot \left[F_m^{\nu} \exp\left(-jk_{zm}^{\nu} z\right) + B_m^{\nu} \exp\left(+jk_{zm}^{\nu} z\right)\right] \tag{1}$$

from which the transverse field components are derived.

$$E_y^{\nu} = \frac{\partial A_{hz}^{\nu}}{\partial x} \quad , \quad H_x^{\nu} = \frac{-1}{j\omega\mu}\frac{\partial^2 A_{hz}^{\nu}}{\partial x \partial z} \tag{2}$$

In (1) and (2), ν denotes the region, m is the mode number, F and B are forward and backward traveling wave amplitudes, respectively, k_z is the propagation constant, and the impedance is defines as $Z_h = \omega\mu / k_z$.

At input (or output) ports, we have to solve a discontinuity between two dielectric filled waveguides at a magnetic wall interface (Fig. 1, location A). (Note that the magnetic wall interface is chosen initially due to the fact that in a real SIW, there would be an open substrate with microstrip ports.) Let index m denote the modes in region $\nu = -1$ and index k the ones in region $\nu=0$, then after multiplying with the respective orthogonal mode functions [12], we obtain the following coupling elements

$$J_{m,k} = \frac{2}{\sqrt{a_{-1} a_0}} \int_{x_{-1}}^{x_{-1}+a_{-1}} sin\left\{ \frac{m\pi}{a_{-1}} (x - x_{-1}) \right\} \cdot sin\left\{ \frac{k\pi}{a_0} \left(x + \frac{a_0}{2} \right) \right\} dx \tag{3}$$

where the origin in x direction is assumed at the center of the substrate (Fig. 1). After combining matrix $\boldsymbol{J}$ with the frequency-dependent impedance terms:

$$\boldsymbol{M} = Diag\left\{ \sqrt{Y_{hm}^{-1}} \right\} (\boldsymbol{J}) \, Diag\left\{ \sqrt{Z_{hk}^{0}} \right\} \tag{4}$$

the modal scattering matrix of the discontinuity is obtained as

$$\begin{aligned}
\boldsymbol{S}_{11} &= \left[\boldsymbol{M}\boldsymbol{M}^T + \boldsymbol{U} \right]^{-1} \left[\boldsymbol{M}\boldsymbol{M}^T - \boldsymbol{U} \right] \\
\boldsymbol{S}_{12} &= 2\left[\boldsymbol{M}\boldsymbol{M}^T + \boldsymbol{U} \right]^{-1} \boldsymbol{M} = \boldsymbol{S}_{21}^T \\
\boldsymbol{S}_{21} &= \boldsymbol{M}^T \left[\boldsymbol{U} - S_{11} \right] = \boldsymbol{S}_{12}^T \\
\boldsymbol{S}_{22} &= \boldsymbol{U} - \boldsymbol{M}^T \boldsymbol{S}_{12}
\end{aligned} \tag{5}$$

where $\boldsymbol{U}$ denotes the unit matrix.

The discontinuity between a dielectric waveguide and a column of square via holes (Fig. 1, location B) is treated similarly, except for the fact that an N-furcated waveguide is obtained if the section contains N-1 via holes. Thus N different coupling integrals are obtained

$$J_{mk}^{n} = \frac{2}{\sqrt{a_0 a_n}} \int_{x_n}^{x_n + a_n} sin\left\{ \frac{m\pi}{a_0} \left(x + \frac{a_0}{2} \right) \right\} \cdot sin\left\{ \frac{k\pi}{a_n} (x - x_n) \right\} dx \tag{6}$$

with their frequency-depending extensions:

$$\boldsymbol{M}^n = Diag\left\{ \sqrt{Y_{hm}^{0}} \right\} (\boldsymbol{J}) \, Diag\left\{ \sqrt{Z_{hk}^{n}} \right\}. \tag{7}$$

By combining all matrices $\boldsymbol{M}^n$ in a single matrix $\boldsymbol{M}$:

$$\boldsymbol{M} = \left[\boldsymbol{M}^1 \quad \boldsymbol{M}^2 \quad \ldots \quad \boldsymbol{M}^N \right], \tag{8}$$

the modal scattering matrix is obtained as in (5).

Properly cascading all scattering matrices of discontinuities with those of individual homogeneous sections [12]:

$$D^n = Diag\left\{ exp\left(-j k_{zk}^{n} L_n \right) \right\} \tag{9}$$

provides the modal scattering matrix of the entire component.

Situations of overlapping vias, such as in Fig. 1 at location C, arising from the optimization of the positions of vias are dealt with in two different ways. If vias are out of line, then individual via sections are segmented with vanishing lengths between them. If vias overlap in vertical direction, then the number N of subsections is reduced accordingly. If necessary, such overlaps are removed before the final fine-optimization run.

Finally, for fabrication and prototyping, the square via holes have to be converted to circular ones as shown in Fig. 2. Among the several conversions attempted, the one replacing the square via by a circular one whose diameter is the arithmetic mean of the side lengths of its inscribed (a_i) and circumscribed (a_o) squares [13]

$$d = 2a \Big/ \left(1 + 1 \big/ \sqrt{2} \right) \tag{10}$$

has provided the best results in all our designs.

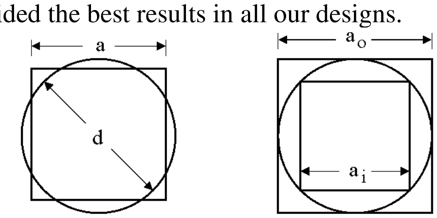

Fig. 2. Square-to-circular via conversion.

Note that this method can be extended to include microstrip ports [14], multiple input and output ports [13], T-junctions and corners [15] as well as losses within waveguide sections.

III. Results

In order to demonstrate the capability of the MMT, Fig. 3 and Fig. 4 show the responses of two three-resonator filters at 21.5 GHz with a transmission zero above or below the passband, e.g. [16]. The substrate is RT/duroid 6002 with square via holes of side length 0.55 mm (circular diameter 0.644 mm [11]) and via pitch of 1.0 mm. It is obvious that

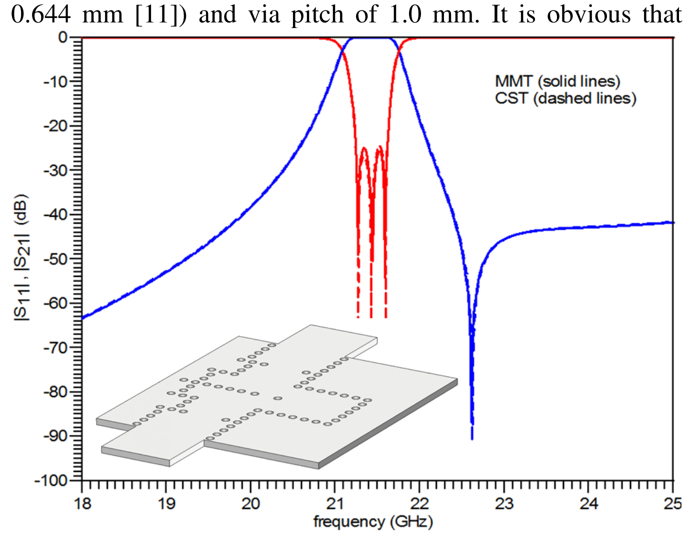

Fig. 3. SIW filter with transmission zero above passband (MMT-square vias, CST-circular vias).

the agreement is quite good despite the fact that the MMT results have been obtained with square vias while CST uses circular vias. Note that dielectric waveguide ports are used in both cases. Slight discrepancies in the return loss responses are attributed to the square-to-circular via conversion. However, since the MMT is at least an order of magnitude faster than CST, depending on code implementation, these small discrepancies are acceptable in favor of a speedy design process. Note that a loss analysis within the MMT (not shown here for lack of space), which has been shown to agree well with CST and measurements, estimates the insertion losses of the two filters in Fig. 3 and Fig. 4 at 1.6 dB and 1.8 dB, respectively.

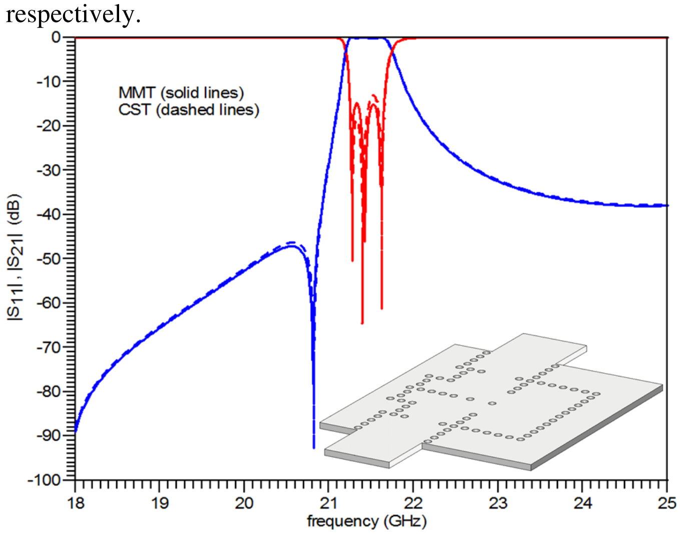

Fig. 4. SIW filter with transmission zero below passband (MMT-square vias, CST-circular vias).

VII. Conclusion

The MMT presents a viable option for the analysis, optimization and design of passive SIW components. A TE_{m0} mode set and an efficient square-to-circular via conversion make the MMT significantly faster than commercially available field solvers which is especially important in (fine-) optimization runs. Two filter designs demonstrate the practicality of the presented approach.

References

[1] F. Xu, Y. Zhang, W. Hong, K. Wu, and T.J. Cui, “Finite-difference frequency-domain algorithm for modeling guided-wave properties of substrate integrated waveguide,” *IEEE Trans. Microw. Theory Tech.*, vol. 51, pp. 2221-2227, Nov. 2003.

[2] F. Xu, K. Wu, and W. Hong, “Domain decomposition FDTD algorithm combined with numerical TL calibration technique and its application in parameter extraction of substrate integrated circuits,” *IEEE Trans. Microw. Theory Tech.*, vol. 54, pp. 329–338, Jan. 2006.

[3] M. Li, L. Du, and R.S. Chen, “Higher-order FETD method combined with domain decomposition algorithm analysis of substrate integrated waveguide structures,” *Proc. Int. Conf. Microw. MM Wave Techn. (ICMMT)*, pp. 621-624, Chengdu, China, May 2010.

[4] E. Arnieri and G. Amendola, “Analysis of substrate integrated waveguide structures based on the parallel-plate waveguide Green’s function,” *IEEE Trans. Microw. Theory Tech*., vol. 56, pp. 1615-1623, July 2008.

[5] X.H. Wu and A.A. Kishk, *Analysis and Design of Substrate Integrated Waveguide Using Efficient 2D Hybrid Method*, Synthesis Lectures on Computational Electromagnetics, Morgan and Claypool, Jan. 2010.

[6] F. Mira, M. Bressan, G. Conciauro, B.G. Martinez, and V.E.B. Esbert, “Fast S-domain modeling of rectangular waveguides with radially symmetric metal insets,” *IEEE Trans. Microw. Theory Tech*., vol. 53, pp.1294-1303, Apr. 2005.

[7] M. Bozzi, L. Perregrini, and K. Wu, “A novel technique for the direct determination of multimode equivalent circuit models for substrate integrated waveguide discontinuities. *Int. J. RF Microw. CAE*, vol. 19, no. 4, pp. 423-433, July 2009.

[8] R. Rezaiesarlak, E. Mehrshahi, and H.R. Sadreazami, “Hybrid of moment method and mode matching technique to study substrate integrated waveguide,” *Proc. Int. Conf. Microw. MM Wave Techn. (ICMMT)*, pp. 1980-1982, Chengdu, China, May 2010.

[9] A. Belenguer, H. Esteban, V.E. Boria, C. Bachiller, and J.V. Morro, “Hybrid mode matching and method of moments method for the full-wave analysis of arbitrarily shaped structures fed through canonical waveguides using only electric currents,” *IEEE Trans. Microw. Theory Tech*., vol. 58, pp. 537-544, Mar. 2010.

[10] E.D. Caballero, H. Esteban, A. Belenguer, and V.E. Boria, “Efficient analysis of substrate integrated waveguide devices using hybrid mode matching between cylindrical and guided modes,” *IEEE Trans. Microw. Theory Tech*., vol. 60, pp. 232-243, Feb. 2012.

[11] Z. Kordiboroujeni and J. Bornemann, “Designing the width of substrate integrated waveguide structures,” *IEEE Microw. Wireless Compon. Lett.*, vol. 23, pp. 518-520, Oct. 2013.

[12] J. Uher, J. Bornemann, and U. Rosenberg, *Waveguide Components for Antenna Feed Systems. Theory and CAD*, Norwood, USA: Artech House, 1993.

[13] Z. Kordiboroujeni, J. Bornemann, and T. Sieverding, “Mode-matching design of substrate-integrated waveguide couplers,” *Proc. Asia-Pacific Int. Symp. Electromagnetic Compatibility*, pp. 701-704, Singapore, May 2012.

[14] J. Bornemann, F. Taringou, and Z. Kordiboroujeni, “A mode-matching approach for the analysis and design of substrate-integrated waveguide components,” *Frequenz*, Vol. 65, pp. 287–292, Sep. 2011.

[15] Z. Kordiboroujeni and J. Bornemann, “Mode-matching analysis and design of substrate integrated waveguide T-junction diplexer and corner filter”, *Int. J. Numer. Model.*, 2015, in press (early view Oct. 2014).

[16] R.M. Kurzrok, “General three-resonator filters in waveguide,” *IEEE Trans. Microw. Theory Tech*., vol. 14, pp. 46-47, Jan. 1966.